HHS Public Access

Author manuscript

ACS Chem Biol. Author manuscript; available in PMC 2021 April 16.

Published in final edited form as:

ACS Chem Biol. 2020 September 18; 15(9): 2331–2337. doi:10.1021/acschembio.0c00553.

Chemical Probes for Blocking of Influenza A M2 WT and S31N Channels

Christina Tzitzoglaki[1], **Kelly McGuire**[2], **Panagiotis Lagarias**[1], **Athina Konstantinidi**[1], **Anja Hoffmann**[3], **Natalie A. Fokina**[5], **Chulong Ma**[4], **Ioannis P. Papanastasiou**[1], **Peter R. Schreiner**[5], **Santiago Vázquez**[6], **Michaela Schmidtke**[3], **Jun Wang**[4], **David D. Busath**[2,*], **Antonios Kolocouris**[1,*]

[1]Section of Pharmaceutical Chemistry, Department of Pharmacy, National and Kapodistrian University of Athens, Panepistimioupolis-Zografou, 15771, Greece

[2]Department of Physiology and Developmental Biology, Brigham Young University, Provo, UT 84602, USA

[3]Jena University Hospital, Department of Medical Microbiology, Section Experimental Virology, Hans Knoell Str. 2, D-07745 Jena, Germany

[4]Department of Pharmacology and Toxicology, College of Pharmacy, University of Arizona, Tucson, AZ 85721, USA

[5]Institute of Organic Chemistry, Justus Liebig University, Heinrich-Buff-Ring 17, 35392 Giessen, Germany

[6]Laboratori de Química Farmacèutica (Unitat Associada al CSIC), Facultat de Farmàcia, and Institute of Biomedicine (IBUB), Universitat de Barcelona, Av. Joan XXIII, 27-31, Barcelona, E-08028, Spain

Abstract

We report on using the synthetic aminoadamantane-CH_2-aryl derivatives **1–6** as sensitive probes for blocking M2 S31N and M2 WT channels as well as virus replication in cell culture. The binding kinetics for M2 S31N channel are very dependent on the length between the adamantane moiety and the first ring of the aryl head group realized in **2** and **3**, and the girth and length of the adamantane adduct realized in **4** and **5**. Study of **1–6** show that, according to MD simulations and MM-PBSA calculations, all bind in the M2 S31N channel with the adamantyl group positioned

*Corresponding Author: A.K.; Tel: (+301) 210-7274834, Fax: (+301) 210 727 4747; ankol@pharm.uoa.gr ; D.D.B.; david_busath@byu.edu,.

C. Tzitzoglaki and K. McGuire contributed equally as co-first authors. A. Kolocouris designed this research project and with D. D. Busath supervised the research. C. Tzitzoglaki did ligand synthesis and MD simulations with OPLS2005. A. Konstantinidi did the docking and with P. I. Lagarias the MM-PBSA calculations. K. McGuire did the EP experiments with compounds **2–5, MD simulations and SMD simulations with CHARMM36. C. Ma and J. Wang did complementary EP experiments with compounds **1** and **6**. N. A. Fokina and P. R. Schreiner prepared aminodiamantane **10** and aminotriamantane **11** and I. P. Papanastasiou 4-(1-adamantyl)aniline **9**. A. Hoffmann in the M. Schmidtke group did the biological testing. S. Vázquez provided research results insights and participated in a relevant ongoing collaboration. A. Kolocouris, D. D. Busath wrote the manuscript and J. Wang, M. Schmidtke, P. R. Schreiner revised it.

Supporting Information.

Methods, eight Figures and nine Tables describing EP results for **1** against the S31 channels of A/Calif/07/2009 M2 N31S and A/Udorn/72 M2 WT, RMSDs from MD simulations, molecular docking and MM-PBSA calculations results, SMD simulations protocol and results.

between V27 and G34 and the aryl group projecting out of the channel with the phenyl (or isoxazole in **6**) embedded in the V27 cluster. In this outward binding configuration, an elongation of the ligand by only one methylene in rimantadine **2**, or using diamantane as well as triamantane insetad of adamantane in **4** and **5**, respectively, causes an incomplete entry and facilitates exit, abolishing effective block compared to the amantadine derivatives **1** and **6**. In the active M2 S31N blockers **1** and **6**, the phenyl and isoxazolyl head groups achieve a deeper binding position, corresponding to high k_{on} / low k_{off} and high k_{on} / high k_{off} measured rate constants, compared to inactive **2–5**, which have much lower k_{on} and higher k_{off}. Compounds **1–5** each block the M2 WT channel by binding in the longer area from V27 - H37, in the inward orientation, with high k_{on} and low k_{off} rate constants. Infection of cell cultures by influenza virus containing M2 WT or M2 S31N is inhibited by **1**–**5** and **1**–**4**, and **6** respectively. While **1** and **6** block infection through the M2 block mechanism in the S31N variant, **2–4** may block M2 S31N virus replication in cell culture through the lysosomotropic effect, just as chloroquine is thought to inhibit SARS-CoV-2 infection.

Graphical Abstract

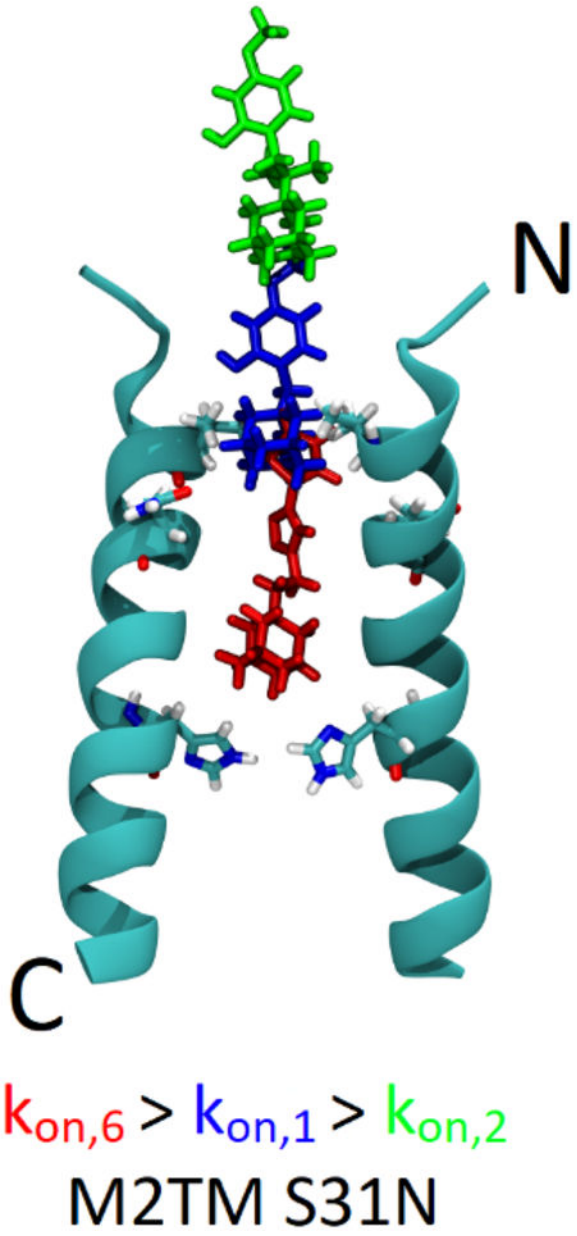

Keywords

aminoadamantane - aryl head group conjugates; anti-viral assay; binding kinetics; electrophysiology; influenza A M2 WT; influenza A M2 S31N; lysosomotropic; MD simulations; MM-PBSA calculations; steered-MD simulations; synthesis

Amantadine variants (aminoadamantanes) can block proton current mediated by the influenza A homotetrameric M2 WT channel,[1–4] abrogating the low pH mediated release of viral ribonuclear proteins from the virus capsid at endosome expulsion.[5] These anti-viral effects result from binding to a high affinity site in the channel lumen, with the adamantyl group at the level of pore-lining residues 30 and 31.[6,7] Outside that site, four V27 residues

form a hydrophobic ring lining the narrow channel entry.[6–8] Deeper inside the channel, four H37 residues form the proton selectivity filter. In M2 WT, amantadine binds at this site with the amine projecting inwards towards the H37 cluster, and the adamantyl group contacting the hydrophobic gate of V27 to seal the channel to water-mediated proton flow. Additionally, amantadine variants, especially those with hydrophobic adducts, can act as lysosomotropic drugs,[9] which accumulate in intracellular vesicles through membrane permeation by the electroneutral form and increase intravesicular pH, causing endosome and/or trans-Golgi network neutralization and inhibition of viral reproduction.[10] Noteworthy, SARS-CoV-2 is inhibited by chloroquine, probably because it acts as a lysosomotropic drug.[11]

Resistance of influenza A virus (IAV) to the proton channel drugs amantadine and rimantadine is associated with mutations in the M2 transmembrane domain (M2TM). The vast majority of resistant viruses (95%) bear the S31N substitution in M2.[12] The M2 S31N mutant, which is currently the main epidemic strain, is a naturally occurring amantadine- and rimantadine-resistant mutation that otherwise maintains channel function nearly identical to the M2 WT, refering to the strain A/Udorn/72 commonly used in electrophysiology (EP) studies.

DeGrado and Wang discovered potent compounds acting against M2 S31N in both EP and antiviral assays.[13–17] These compounds are second generation amantadine-based drug molecules, which include aryl or heteroaryl rings (as war heads) linked with amantadine through a methylene bridge. Extensive structure-activity relationships (SAR) investigations on activity and/or binding kinetics were performed through modifications of the adamantyl group and the aryl head group.[13–17] Scheme 1 shows the dual channel-type inhibitor **1** with a 2-hydroxy-4-methoxy-phenyl group,[14] one of the simpler aryl head groups in structure, which blocks both M2 WT and M2 S31N channels, and **6** with a 3-(2-thiophenyl)-isoxazolyl group, which only blocks the M2 S31N channel.[13] DeGrado and Hong showed that for complexes of M2TM S31N with **6** or analogues in DPC micelles (using solution NMR combined with MD simulations),[13,15] and in DMPC lipid bilayers (using solid state NMR),[18] the adamantane moiety of the drug is bound in the pore between N31 and G34 while the aryl tail projects through the Val27 side chains. This outward orientation in the M2 S31N channel is opposite from the inward orientation of amantadine in the M2 WT channel.[7,8] DeGrado and Wang also discovered, using solution NMR in micelles and MD simulations, that a dual channel-type inhibitor, similar to compound **1** but consisting of a 2-bromo-thiophenyl group connected with amantadine through a methylene, is oriented with the aryl head group outward in the M2TM S31N and inward in the M2TM WT pore.[15] The second generation amantadine-based drugs can block M2 S31N with association/dissociation rate constants (k_{off}/k_{on}) that are slow off/fast on or slow off/slow on leading to favorable $K_d = k_{off}/k_{on}$ values and antiviral potency.[16,17]

The kinetics of a ligand binding to its protein target are seen as increasingly important for *in vivo* efficacy in drug discovery[19] and are critical for amantadine - aryl head conjugates.[16,17] A targeted optimization of binding kinetics is difficult to achieve and requires systematic studies, also needed for M2 channels, to increase the understanding about molecular interactions involved.[17] Here, we used the comparable but distinctive ligands **1–6** (Scheme

1) that expand on the structural motifs in **1**[14] and **6**,[13] as a set of useful chemical probes for exploring the molecular features affecting the energetics, orientational trajectory, kinetics of blocking of M2 WT and S31N channels, as well as alternative mechanisms of inhibition such as potential lysosomotropic behavior.

Synthetic Chemistry.

In the designed chemical probes, the linker between the adamantane and amino group, is CMe_2 (isopropyl) in **2** or phenyl in **3**. The impact of using a larger non-polar component, was explored with diamantanyl in **4** and triamantanyl in **5**. Compared to **1**, amantadine **7** is replaced with 2-(1-adamantyl)-propan-2-amine **8** in **2**, 4-(1-adamantyl)-1-benzenamine **9** in **3**, 4-aminodiadamantane **10** in **4**, and 9-aminotriadamantane **11** in **5**, respectively.

The reaction of **7–11** with 2-hydroxy-4-methoxy-benzaldehyde using $NaCNBH_3$ in methanol for 15 min, afforded the corresponding imines **11–15**. The reduction gave the amines **1–5** upon treatment of the imine first with p-toluenesulfonic acid (PTSA) and then with $NaBH_4$ in methanol (Scheme 1) (for the synthetic procedures, see the Supporting Information).

In vitro testing.

We applied the cytopathic effect (CPE) inhibition assay[20] to compare the antiviral activity of **1–6** against the A/WSN/33 virus (with naturally occurring M2 N31) and the A/WSN/33 M2 N31S virus, which was generated by reverse genetics from A/WSN/33.[21]

Compounds **1–4** have low micromolar or submicromolar potency, similar to amantadine or rimantadine,[22] inhibiting the amantadine-sensitive A/WSN/33 M2 N31S (M2 WT) replication at concentations 0.09 – 1.13 μM (WT, Table 1), while **5** has a mediocre antiviral activity (8.10 μM). As expected, the oseltamivir control demonstrates that the genetically engineered M2 mutant virus remains vulnerable to the potent neuraminidase inhibitor. Against amantadine-resistant A/WSN/33 (with M2 N31), only **6** has sub-micromolar potency, but **1**–**4** show mediocre activity. Compound **3** is as effective as the dual-inhibitor **1**, and therefore also classifiable as a dual channel-type.[14] The moderate potency of **1** and high potency of **6** against the amantadine-resistant virus M2 S31N found here is consistent with previous results by Wang and DeGrado.[13–17]

TEVC experiments.

Using two-electrode voltage clamp (TEVC), we calculated %-block at 10 min of 100 μM drug perfusion (Tables 2 and 3) to obtain more reliable results, as we recently suggested, [17,23,24] compared to the 2-min perfusion usually used.[13–17] We found that molecules **1–5** strongly block the M2 WT channel-mediated proton current (Tables 2 and S1) whereas **6** has almost no potency, and that **1** and **6** produce high 10-min %-block of M2 S31N. In constrast, **2** being over 30-fold more potent in blocking M2 WT current than **1**, and moderately effective in vitro against the M2 S31N bearing influenza virus strain A/WSN/33, it is strikingly impotent against M2 S31N in the EP assay of molecular function, indicating that the simple isopropyl linker eliminates potency in this M2 S31N environment (Table 3). Also,

3–5, which inhibit A/WSN/33 replication in cell culture at dosages similar to **1**, do not effectively block proton currents through M2 S31N expressed in oocytes (Table 3).

To quantitate the kinetics of the block and unblock processes using EP in oocytes, we evaluated the association and dissociation rate constants from the exponential block and unblock rates associated with the equilibrium relaxation, and then calculated K_d from the k_{off}/k_{on} ratio.[16,17] These rate constants allow one to examine the ease of exit and entry. For one set of seven compounds that block M2 S31N efficiently, it was previously observed that six of the compounds have k_{on} values range from 29 to 227 $M^{-1}s^{-1}$ and k_{off} values range from 0.3–1.5 × 10^3 s^{-1},[17] i.e., these compounds have fast on/slow off or slow on/slow off, [16,17] with the kinetics of binding being very dependent on the adamantane scaffold but also on the aryl head group.[17] In the 7th compound of that series, the aryl head was changed from an azole-like heterocycle to a phenyl-SiR_3 group which cannot form hydrogen bonding interactions with the mouth of the channel, and k_{on} increased to 691 $M^{-1}s^{-1}$ and the k_{off} to 10.3 × 10^{-3} s^{-1}.[17]

Compound **1** and its four variants **2–5**, show significant blocking of inward current in the M2 WT channel (Table 2), with high percent blocking, low percent washout, high association rate k_{on}, and low dissociation rate k_{off}. The k_{on} values of **1–5** for M2 WT are in the range 84–381 $M^{-1}s^{-1}$ and the k_{off} values are in the range 0.56–5.10 × 10^{-3} s^{-1} and thus, **1–5** are fast on / slow off, with **2–5** having higher k_{on} than **1** by >4. Evidently, the elongation of the distance between the aryl head group and the adamantyl moiety in **2** and **3** or the 14-carbon diamantane and the 18-carbon triamantane facilitate both entry and dwell time and fit into the M2TM WT pore and block the M2 WT channel, with **5** being probably the bulkiest M2 WT channel blocker found yet (Table 2). The converged MD simulations (Figure S3) of the complexes in DMPC bilayers show that compounds **1–6** bind in M2 WT in the region spanning from V27 to H37, with the ammonium hydrogen bonding with waters and G34 carbonyls and the adamantane moiety in contact with V27 side chains (Figures 1A, 1C, S1A, S2). Calculated free energies of binding based on MD simulations and the MM-PBSA method (Table S5), as well as simple rigid-body docking (Table S4), show that **1–6** bind to M2 WT with the inward orientation, i.e., with a more negative binding free energy for the inward orientation (see ΔG_{eff} values from MM-PBSA method in Table S5) compared to the outwardly projecting orientation. (For energy decompositions, see Tables S6–S9).

In the M2 S31N channel (Table 3), the percent inward current blockage by compounds **2–5** is significantly reduced (compared to WT, Table 2), and also very dependent on the linker between adamantane and the aryl head group, with compound **2** showing no measurable block. The reduction in %-block for compounds **3–5** is due to a 5- to 10-fold reduction in k_{on}, and 10- to 30-fold increase in k_{off} (slow on / fast off). Therefore, with low association rates and high dissociation rates, the dissociation constant K_d calculated from the fitted rate constants is above 100 μM for compounds **3–5**, a low binding affinity. The k_{on} of **1** for M2 S31N is 124 $M^{-1}s^{-1}$ and k_{off} is 2.6 × 10^{-3} s^{-1}. Thus, **1** is fast on / slow off while **6** is very fast on / fast off.

As a contrasting case, we tested **6**, a known blocker of M2 S31N.[3] As found previously,[3] **6** shows significant blocking of the S31N channel, with almost complete blocking of inward

current and low percent washout. The percent-washout and the slow k_{off} are similar to those of compounds **3** and **4** (Figures S6–S8), but the k_{on} is very high and complete (99.2%) blocking is attained, such that **6** has high potency in blocking M2 S31N, as well as in blocking cell infection for the M2 S31N virus.[13] Indeed, perhaps the most intriguing result in this SAR on binding kinetics is the remarkably high k_{on} (2280 $M^{-1}s^{-1}$) for **6** in the S31N, ca. 10- to 100-fold higher, than others tested to date,[13–17] which have "high" k_{on} values such as ca. 230 $M^{-1}s^{-1}$ [17] (Table 3). Although k_{on} is still 6–7 orders of magnitude lower than expected for unhindered diffusion-limited binding,[26,27] the association rate constant is much higher than that observed for **1** in S31N, or for **2**–**5** in WT (Table 2). The entry rate of **6** into M2 WT is even faster (Table 2, footnote h), but the exit rate from M2 WT is dramatically faster still, resulting in non-efficient block. Note that for **6**, an inhibitor of M2 S31N but not M2 WT, the aryl head group consists of the polar isoxazole ring linked with a hydrophobic thiophenyl ring, while in **1**, which blocks both M2 isoforms,[14,15] it consists of the apolar 4-methoxy group attached to a 2-hydroxyl-phenyl ring.

The converged MD simulation trajectories of the M2 S31N complexes in DMPC bilayers (Figure S4), show that the ligands bind as a whole, more outwardly in the channel, compared to the M2 WT pore, in the region between V27 and G34 with the aryl adduct facing outward and projecting through the V27 cluster (Figures 1B and 1D, S1B) (see PDB ID 2LY0[13]). The adamantane moiety is positioned deeper in the channel from N31 side chains, between G34 and A30 (Figures 1B, 1D), while the ammonium group and the polar part of the aryl head (2-hydroxyl group connected with 4-methoxy-phenyl in **1–5** or oxazole in **6**) form hydrogen bonds with N31 side chains and waters (Figures 1B, 1D, S1B, S5 and details in the Supporting Information), which may guide association, consistent with the lower calculated desolvation penalty compared to the M2 WT complexes (Tables S6–S9). The V27 side chain cluster is tightly packed around the 4-methoxy in **1, 4**, and **5**, but around the 2-hydroxy-4-methoxy-phenyl in **2** and **3**, and between oxazole and thiophenyl rings in **6**. In this outward binding configuration, an elongation of the ligand by only one isopropyl in rimantadine **2**, by a phenyl group in **3**, and the expanded diamondoid substructures instead of adamantyl in **4** and **5**, respectively, seems to cause an incomplete entry, according to the kinetics observed with TEVC (Tables 2, 3) which showed, as previously described, slow entrance (reduced k_{on} constants) and fast escape rates (increased k_{off}) for **2–5** in S31N (Table 3) or **6** in M2 WT, compared to **1–5** in WT (Table 2) and **1** or **6** with M2 S31N (Table 3).

EC_{50} values for the A/WSN/33 (M2 N31) and A/WSN/33 M2 N31S constructs represented in Table 1 can be compared and contrasted with K_d values in the last columns of Tables 2 and 3, respectively. Compounds **2**–**4** have moderately high anti-viral efficacies (8 – 21 μM) against A/WSN/33 in MDCK cell culture (Table 1) in the face of inefficient M2 S31N block, it is clear that **2**–**4** can also block influenza virus by another mechanism. Additionally the previously reported IC_{50} for **6** in TEVC with M2 S31N is 16 μM,[13] similar to the K_d found here, 7.5 μM. At the same time, these authors found a much lower EC_{50} using the plaque reduction assay for the antiviral activity of **6** against A/WSN/33, ca 0.1 μM, similar to that found here in the cytopathic effect assay, 0.153 μM (Table 1). Compounds **1–5** have K_ds from EP ranging between 1 and 10 μM, more similar to amantadine, which blocks M2 WT with an apparent K_i of 0.3 μM,[2] and EC_{50}s 0.09 – 1.13 μM. The difference of magnitude

between the anti-viral potency and the channel inhibition constant, which is more significant for M2 S31N virus growth inhibition is not understood, but may suggest additional mechanisms of anti-viral activity, plausibly a lysosomotropic effect, as observed previously by Scholtissek,[10] Busath and Kolocouris,[28] and Naesens and Vazquez[29] for amantadine variants with lipophilic adducts inhibiting virus at concentrations higher than c.a. 20 μM.[10,30] Thus, these compounds can always buffer late-stage endosomes to prevent acid-induced fusion of the virus envelope with the endosome membrane.[31] Such lysosomotropic agents are effective against many types of viruses *in vitro*, including the coronavirus SARS-CoV-2.[11]

In conclusion, here we describe the effect of ligand's structure on binding kinetics for M2 WT and S31N channels using the synthetic aminoadamantane-CH_2-aryl derivatives **1**–**6** as chemical probes. Noteworthy, only the binding kinetics for M2 S31N channel are very dependent on the length between the adamantane moiety and the first ring of the aryl head group realized in **2** and **3**, and the girth and length of the adamantane adduct realized in **4** and **5**.

Supplementary Material

Refer to Web version on PubMed Central for supplementary material.

Acknowledgements.

Chiesi Hellas fully supported the Ph.D thesis of C. Tzitzoglaki (SARG No 10354) and the State Scholarships Foundation (IKY) provides a Ph.D fellowship to P. Lagarias (MIS 5000432, NSRF 2014-2020). NIH grant supports the work of J. Wang group. A. Kolocouris and S. Vázquez thank Fundació La Marató de TV3 for finantial support. The National HPC facility, ARIS, under Greek Research & Technology Network (GRNET) and project (IDs pr002021) and the Fulton Supercomputer at the BYU Office of Research Computing provide super computer time.

Abbreviations.

CPE	Cytopathic effect
COM	center of mass
DMPC	dimirystoyl-*sn*-glycero-3-phosphocholine
EP	electophysiology
IAV	influenza A virus
MD	molecular dynamics
PME	particle mesh Ewald method
PDB	protein data bank
RESPA	reversible multiple time scale molecular dynamics
RMSD	root-mean-square deviation
SMD	steered-MD

PTSA	p-toluenesulfonic acid
M2TM	transmembrane domain of the M2 protein
WT	wild type

References

(1). Skehel JJ; Hay AJ; Armstrong JA On the Mechanism of Inhibition of Influenza Virus Replication by Amantadine Hydrochloride. J. Gen. Virol 1978, 38, 97–110. [PubMed: 563896]

(2). Wang C; Takeuchi K; Pinto LH; Lamb RA Ion Channel Activity of Influenza A Virus M2 Protein: Characterization of the Amantadine Block. J. Virol 1993, 67, 5585–5594. [PubMed: 7688826]

(3). Jing X; Ma C; Ohigashi Y; Oliveira FA; Jardetzky TS; Pinto LH; Lamb RA Functional Studies Indicate Amantadine Binds to the Pore of the Influenza A Virus M2 Proton-Selective Ion Channel. Proc. Natl. Acad. Sci. U. S. A 2008, 105, 10967–10972. [PubMed: 18669647]

(4). Pinto LH; Holsinger LJ; Lamb RA Influenza Virus M2 Protein Has Ion Channel Activity. Cell 1992, 69, 517–528. [PubMed: 1374685]

(5). Bui M; Whittaker G; Helenius A Effect of M1 Protein and Low PH on Nuclear Transport of Influenza Virus Ribonucleoproteins. J. Virol 1996, 70, 8391–8401. [PubMed: 8970960]

(6). Stouffer AL; Acharya R; Salom D; Levine AS; Di Costanzo L; Soto CS; Tereshko V; Nanda V; Stayrook S; DeGrado WF Structural Basis for the Function and Inhibition of an Influenza Virus Proton Channel. Nature 2008, 451, 596–599. [PubMed: 18235504]

(7). Thomaston JL; Polizzi NF; Konstantinidi A; Wang J; Kolocouris A; DeGrado WF Inhibitors of the M2 Proton Channel Engage and Disrupt Transmembrane Networks of Hydrogen-Bonded Waters. J. Am. Chem. Soc 2018, 45, 15219–15226.

(8). Cady SD; Wang J; Wu Y; Degrado WF; Hong M Specific Binding of Adamantane Drugs and Direction of Their Polar Amines in the Pore of the Influenza M2 Transmembrane Domain in Lipid Bilayers and Dodecylphosphocholine Micelles Determined by NMR Spectroscopy. J. Am. Chem. Soc 2011, 133, 4274–4284. [PubMed: 21381693]

(9). Pisonero-Vaquero S; Medina DL Lysosomotropic Drugs: Pharmacological Tools to Study Lysosomal Function. Curr. Drug Metab 2017, 18, 1147–1158. [PubMed: 28952432]

(10). Scholtissek C; Quack G; Klenk HD; Webster RG How to Overcome Resistance of Influenza A Viruses against Adamantane Derivatives. Antiviral Res 1998, 37, 83–95. [PubMed: 9588841]

(11). Wang M; Cao R; Zhang L; Yang X; Liu J; Xu M; Shi Z; Hu Z; Zhong W; Xiao G Remdesivir and Chloroquine Effectively Inhibit the Recently Emerged Novel Coronavirus (2019-NCoV) in Vitro. Cell Res 2020, 30, 269–271. [PubMed: 32020029]

(12). Garcia V; Aris-Brosou S Comparative Dynamics and Distribution of Influenza Drug Resistance Acquisition to Protein M2 and Neuraminidase Inhibitors. Mol. Biol. Evol 2014, 31, 355–363. [PubMed: 24214415]

(13). Wang JJ; Wu Y; Ma C; Fiorin G; Pinto LH; Lamb R. a.; Klein ML; Degrado WF Structure and Inhibition of the Drug-Resistant S31N Mutant of the M2 Ion Channel of Influenza A Virus. Proc Natl Acad Sci U S A 2013, 110, 1315–1320. [PubMed: 23302696]

(14). Wang J; Ma C; Wang J; Jo H; Canturk B; Fiorin G; Pinto LH; Lamb RA; Klein ML; DeGrado WF Discovery of Novel Dual Inhibitors of the Wild-Type and the Most Prevalent Drug-Resistant Mutant, S31N, of the M2 Proton Channel from Influenza A Virus. J. Med. Chem 2013, 56, 2804–2812. [PubMed: 23437766]

(15). Wu Y; Canturk B; Jo H; Ma C; Gianti E; Klein ML; Pinto LH; Lamb RA; Fiorin G; Wang J; Degrado WF Flipping in the Pore: Discovery of Dual Inhibitors That Bind in Different Orientations to the Wild-Type versus the Amantadine-Resistant S31N Mutant of the Influenza a Virus M2 Proton Channel. J. Am. Chem. Soc 2014, 136, 17987–17995. [PubMed: 25470189]

(16). Hu Y; Hau RK; Wang Y; Tuohy P; Zhang Y; Xu S; Ma C; Wang J Structure-Property Relationship Studies of Influenza A Virus AM2-S31N Proton Channel Blockers. ACS Med. Chem. Lett 2018, 9, 1111–1116. [PubMed: 30429954]

(17). Wang Y; Hu Y; Xu S; Zhang Y; Musharrafieh R; Hau RK; Ma C; Wang J In Vitro Pharmacokinetic Optimizations of AM2-S31N Channel Blockers Led to the Discovery of Slow-Binding Inhibitors with Potent Antiviral Activity against Drug-Resistant Influenza A Viruses. J. Med. Chem 2018, 61, 1074–1085. [PubMed: 29341607]

(18). Williams JK; Tietze D; Wang J; Wu Y; Degrado WF; Hong M Drug-Induced Conformational and Dynamical Changes of the S31N Mutant of the Influenza M2 Proton Channel Investigated by Solid-State NMR. J. Am. Chem. Soc 2013, 135, 9885–9897. [PubMed: 23758317]

(19). Vauquelin G Effects of Target Binding Kinetics on in Vivo Drug Efficacy: Koff , Kon and Rebinding. Br J Pharmacol 2016, 173, 2319–2934. [PubMed: 27129075]

(20). Schmidtke M; Schnittler U; Jahn B; Dahse H-M; Stelzner A A Rapid Assay for Evaluation of Antiviral Activity against Coxsackie Virus B3, Influenza Virus A, and Herpes Simplex Virus Type 1. J. Virol. Methods 2001, 95, 133–143. [PubMed: 11377720]

(21). Hoffmann E; Neumann G; Kawaoka Y; Hobom G; Webster RG A DNA Transfection System for Generation of Influenza A Virus from Eight Plasmids. Proc. Natl. Acad. Sci 2000, 97, 6108–6113. [PubMed: 10801978]

(22). Drakopoulos A; Tzitzoglaki C; Ma C; Freudenberger K; Hoffmann A; Hu Y; Gauglitz G; Schmidtke M; Wang J; Kolocouris A Affinity of Rimantadine Enantiomers against Influenza A/M2 Protein Revisited. ACS Med. Chem. Lett 2017, 8, 145–150. [PubMed: 28217261]

(23). Barniol-Xicota M; Gazzarrini S; Torres E; Hu Y; Wang J; Naesens L; Moroni A; Vázquez S Slow but Steady Wins the Race: Dissimilarities among New Dual Inhibitors of the Wild-Type and the V27A Mutant M2 Channels of Influenza A Virus. J. Med. Chem 2017, 60, 3727–3738. [PubMed: 28418242]

(24). Drakopoulos A; Tzitzoglaki C; McGuire K; Hoffmann A; Konstantinidi A; Kolokouris D; Ma C; Freudenberger K; Hutterer J; Gauglitz G; Wang J; Schmidtke M; Busath DD; Kolocouris A Unraveling the Binding, Proton Blockage, and Inhibition of Influenza M2 WT and S31N by Rimantadine Variants. ACS Med. Chem. Lett 2018, 9, 198–203. [PubMed: 29541360]

(25). Li F; Ma C; Hu Y; Wang Y; Wang J Discovery of Potent Antivirals against Amantadine-Resistant Influenza A Viruses by Targeting the M2-S31N Proton Channel. ACS Infect. Dis 2016, 2, 726–733. [PubMed: 27657178]

(26). Alberty RA; Hammes GG Application of the Theory of Diffusion-Controlled Reactions to Enzyme Kinetics. J. Phys. Chem 1958, 62, 154–159.

(27). Chou KC; Zhou GP Role of the Protein Outside Active Site on the Diffusion-Controlled Reaction of Enzyme. J. Am. Chem. Soc 1982, 104, 1409–1413.

(28). Kolocouris A; Tzitzoglaki C; Johnson FB; Zell R; Wright AK; Cross TA; Tietjen I; Fedida D; Busath DD Aminoadamantanes with Persistent in Vitro Efficacy against H1N1 (2009) Influenza A. J. Med. Chem 2014, 57, 4629–4639. [PubMed: 24793875]

(29). Torres E; Fernández R; Miquet S; Font-Bardia M; Vanderlinden E; Naesens L; Vázquez S Synthesis and Anti-Influenza a Virus Activity of 2,2-Dialkylamantadines and Related Compounds. ACS Med. Chem. Lett 2012, 3, 1065–1069. [PubMed: 24900429]

(30). Konstantinidi A; Naziris N; Chountoulesi M; Kiriakidi S; Sartori B; Kolokouris D; Amentisch H; Mali G; Ntountaniotis D; Demetzos C; Mavromoustakos T; Kolocouris A Comparative Perturbation Effects Exerted by the Influenza A M2 WT Protein Inhibitors Amantadine and the Spiro[Pyrrolidine-2,2′-Adamantane] Variant AK13 to Membrane Bilayers Studied Using Biophysical Experiments and Molecular Dynamics Simulations. J. Phys. Chem. B 2018, 122, 9877–9895. [PubMed: 30285441]

(31). Helenius A Unpacking the Incoming Influenza Virus. Cell 1992, 69, 577–578. [PubMed: 1375129]

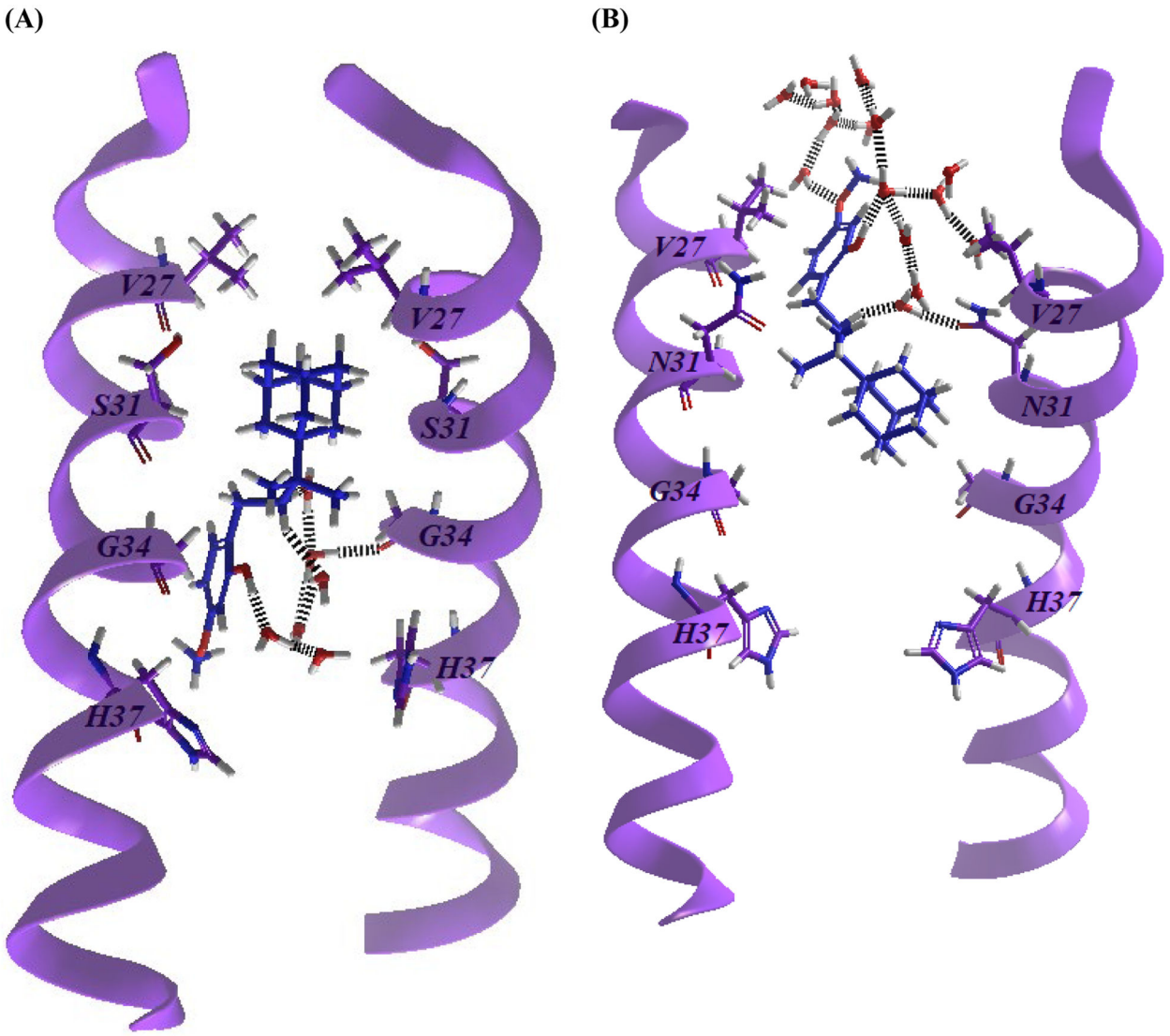

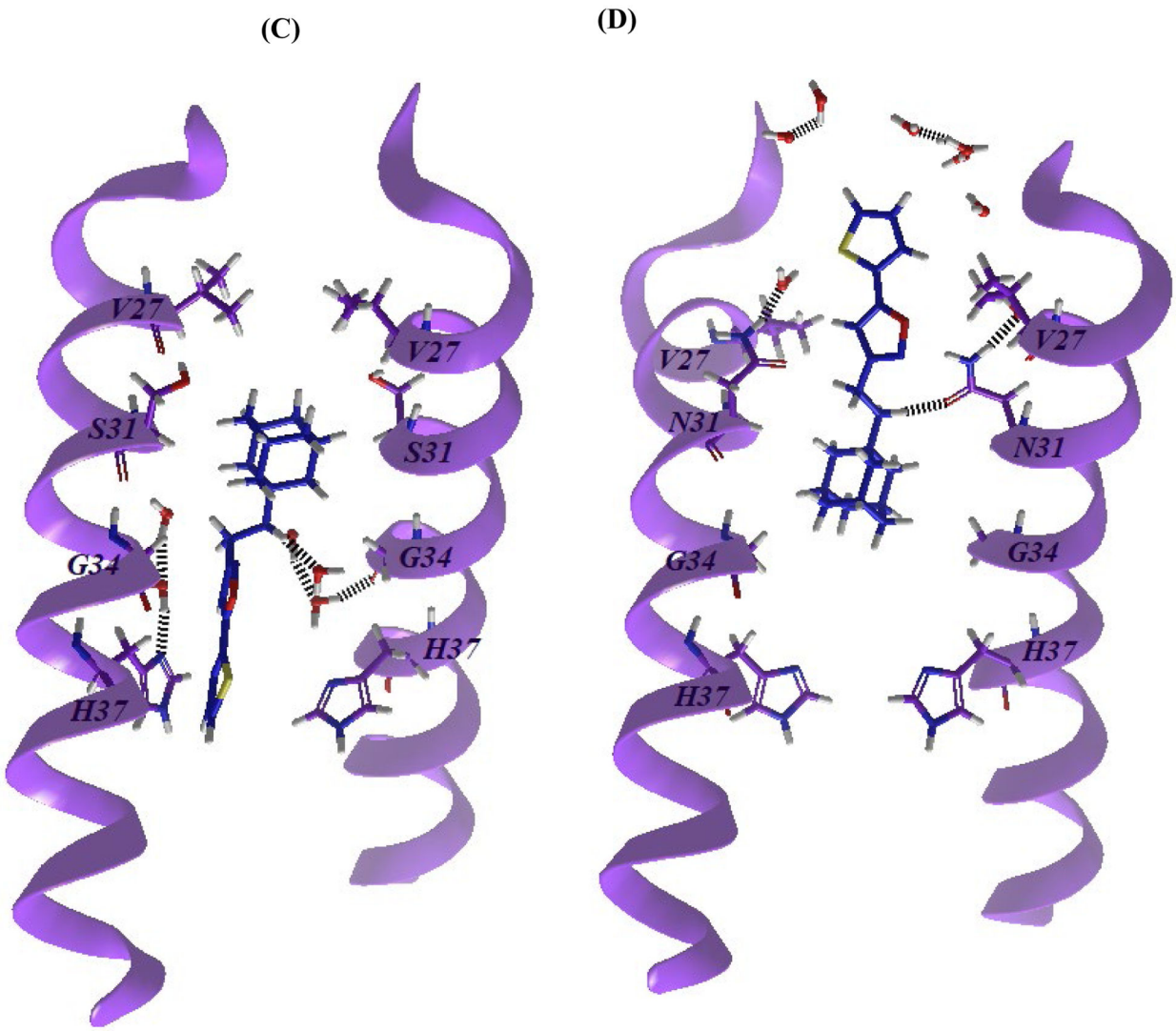

Figure 1.

Snapshots of ligand-protein complexes in hydrated DMPC after 80 ns MD simulation using the amber14sb force field (1 atm, 310 K). Compound **2** bound to (A) M2TM WT (PDB ID 2KQT) with a preferred inward orientation, or (B) M2TM (PDB ID 2KQT) S31N with a preferred outward orientation. Compound **6** bound to M2TM WT (PDB ID 2KQT) with a preferred inward orientation (C) or M2TM (PDB ID 2KQT) S31N with a preferred outward orientation. (D) See Table S5 for orientation preference energies.

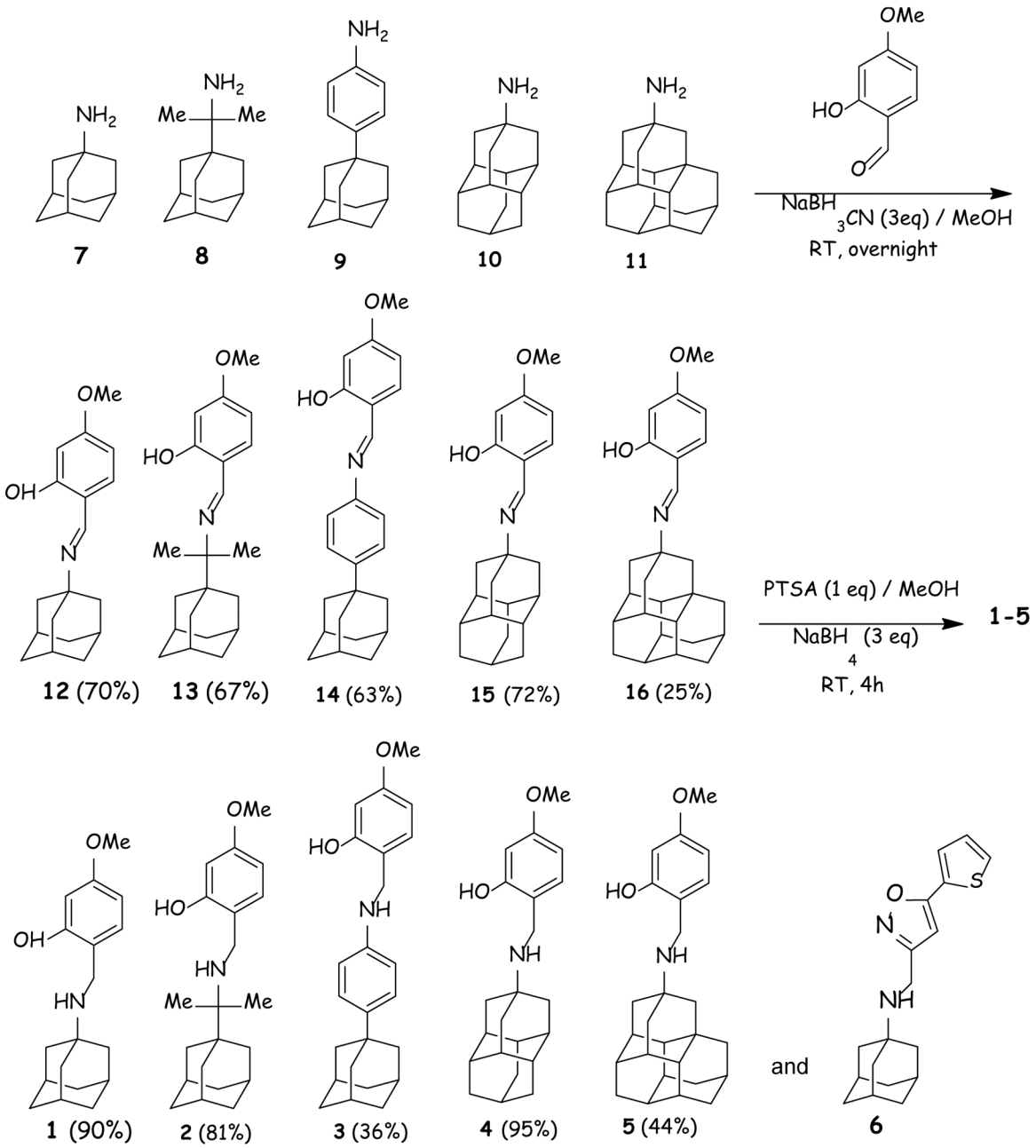

Scheme 1.

Structures of compounds **1–6** used as chemical probes to investigate binding to M2 WT and M2 S31N channels. The upper part shows the reductive amination procedure applied for the synthesis of aminoadamantane derivatives **1–5** through imines **12–16**, starting from the corresponding amines **7–11**.

Table 1.

In vitro cytotoxicity (CC_{50}, μM) and efficacy (EC_{50}, μM) of compounds **1–6** tested against initial cell infection (CPE inhibition assay) in MDCK cells

	CC_{50} ± SD [μM]	EC_{50} ± SD [μM]	
Compound	**MDCK cells**	**A/WSN/33 M2 N31S**	**A/WSN/33 (M2 N31)**
1	49.86 ± 12.28	1.13 ± 0.03	8.74 ± 4.6
2	>100	0.09 ± 0.005	20.93 ± 9.05
3	>100	0.66 ± 0.21	8.04 ± 2.43
4	>100	0.29 ± 0.11	22.01 ± 14.67
5	27.13 ± 9.43	8.10 ± 2.72	not active
6	not tested	not active	0.153 μM
Amantadine[a]	not tested	0.25 ± 0.07	not active
Oseltamivir[a]	not tested	0.03 ± 0.02	0.01 ± 0.01

[a]control compounds

Table 2.

Block of full-length A/Udorn/72 M2 WT current by compounds **1–6**.

Compound	Conc.	Sample Size	Percent Block (%)[a]	Blockage Eliminated in Wash Out(%)[b]	k_{on} ($M^{-1}s^{-1}$)[c,f]	$10^3 \times k_{off}$ (s^{-1})[d,f]	K_d(μM)[e]
1	100 μM	N = 3	64 ± 1	48 ± 1	84.0 ± 9.9	5.1±0.32	60.5 ± 10.4
2	100 μM	N = 3	77 ± 2	0.5 ± 0.1	332.6 ± 1.7	0.56±0.03	1.7 ± 0.6
3	100 μM	N = 3	80 ± 2	1.3 ± 0.2	381.7 ± 1.4	1.7± 0.2	4.5 ± 0.7
4	100 μM	N = 3	81 ± 2	2.1 ± 0.8	378.2 ± 1.1	2.1 ± 0.7	5.6 ± 0.3
5	100 μM	N = 3	81 ± 2	3.1 ± 0.6	377.3 ± 2.1	3.8 ± 0.5	10.1 ± 1.2
6	100 μM	N = 3	11 ± 1[g]	ND[h]	ND	ND	>100

[a] Mean ± SEM calculated at 10 min of drug perfusion

[b] Mean ± SEM calculated at 5 min of washout; percent of original current that returned during washout

[c] Mean ± SEM of exponential fit rate constants obtained from the first two minutes of drug perfusionThis equilibrium relaxation rate constant divided by the compound concentration in the bath is actually an upper limit on the compound's association rate constant (see methods section)

[d] Mean ± SEM of exponential fit rate constants obtained from the first three minutes of washout

[e] Calculated from the ratio, k_{off}/k_{on}

[f] Blockage after 10 min of drug perfusion, blockage eliminated after 5 min of washout, k_{on} is the relaxation rate constant from fit of the 3-min compound perfusion trace, k_{off} is the relaxation rate constant from fit of the 5-min compound washout trace

[g] Taken from ref. 3 as the mean ± SEM calculated at 2 min of drug perfusion

[h] Not determined. The small amount of block of M2 WT by **6** observed was so fast that it was limited by perfusion rate, judging by the rate of ungating upon return to alkaline solution, and the extent of block at 100 μM (11%) suggests a K_d ~ 900 μM and thus a $k_{off} > 1\ s^{-1}$.

Table 3.

Block of full-length A/Udorn/72 M2 S31N current by compounds **1–6**.

Compound	Conc.	Sample Size	Percent Block[a]	Blockage Eliminated in Wash Out(%)[b]	k_{on} ($M^{-1}s^{-1}$)[c]	$10^3 \times k_{off}$ (s^{-1})[d]	K_d (μM)[e]
1	100 μM	N = 3	59 ± 1[f]	34 ± 1	124 ± 9	2.6 ± 0.2	21.3 ± 2.8
2	100 μM	N = 3	No Block	No Block	No Block	No Block	> 100
3	100 μM	N = 3	30 ± 2	4.8 ± 0.5	<64	18 ± 2.2	> 100
4	100 μM	N = 3	25 ± 2	7.2 ± 0.8	<43	56 ± 1.4	> 100
5	100 μM	N = 3	17 ± 1	1.4 ± 1.1	<29	97 ± 3.6	> 100
6	100 μM	N = 3	99 ± 1	6.8 ± 1.2	2280 ± 150	17 ± 2	7.5 ± 0.3[g]

[a] Mean ± SEM calculated at 10 min of drug perfusion (unmeasurable in **2**)

[b] Mean ± SEM calculated at 5 min of washout; percent of original current that returned during washout

[c] Mean ± SEM of exponential fit rate constants obtained from the first two minutes of drug perfusion. This “equilibrium relaxation rate constant divided by the compound concentration in the bath” is actually an upper limit on the compound’s association rate constant (see methods section). Because the measured k_{off} is relatively high for **3**–**5**, these cases, where the correction for k_{off} would substantially reduce the estimate of k_{on}, are denoted with <

[d] Mean ± SEM of exponential fit rate constants obtained from the first three minutes of washout

[e] Calculated from the ratio, k_{off}/k_{on}

[f] Blockage after 10 min of drug perfusion, blockage eliminated after 5 min of washout, k_{on} is the relaxation rate constant from fit of the 3-min compound perfusion trace, k_{off} is the relaxation rate constant from fit of the 5-min compound washout trace

[g] 16 μM found in ref. 3